

---

# 1×N Block Pattern for Network Sparsity

---

Mingbao Lin<sup>1</sup> Yuchao Li<sup>2</sup> Yuxin Zhang<sup>1</sup> Bohong Chen<sup>1</sup>  
Fei Chao<sup>1</sup> Mengdi Wang<sup>2</sup> Shen Li<sup>2</sup> Jun Yang<sup>2</sup> Rongrong Ji<sup>1,3\*</sup>  
<sup>1</sup>Media Analytics and Computing Lab, Department of Artificial Intelligence,  
School of Informatics, Xiamen University    <sup>2</sup>Alibaba Group  
<sup>3</sup>Institute of Artificial Intelligence, Xiamen University

## Abstract

Though network sparsity emerges as a promising direction to overcome the drastically increasing size of neural networks, it remains an open problem to concurrently maintain model accuracy as well as achieve significant speedups on general CPUs. In this paper, we propose one novel concept of  $1 \times N$  block sparsity pattern (block pruning) to break this limitation. In particular, consecutive  $N$  output kernels with the same input channel index are grouped into one block, which serves as a basic pruning granularity of our pruning pattern. Our  $1 \times N$  sparsity pattern prunes these blocks considered unimportant. We also provide a workflow of filter rearrangement that first rearranges the weight matrix in the output channel dimension to derive more influential blocks for accuracy improvements, and then applies similar rearrangement to the next-layer weights in the input channel dimension to ensure correct convolutional operations. Moreover, the output computation after our  $1 \times N$  block sparsity can be realized via a parallelized block-wise vectorized operation, leading to significant speedups on general CPUs-based platforms. The efficacy of our pruning pattern is proved with experiments on ILSVRC-2012. For example, in the case of 50% sparsity and  $N = 4$ , our pattern obtains about 3.0% improvements over filter pruning in the top-1 accuracy of MobileNet-V2. Meanwhile, it obtains 56.04ms inference savings on Cortex-A7 CPU over weight pruning. Code is available at <https://github.com/lmbxmu/1xN>.

## 1 Introduction

Deep neural networks (DNNs) have substantially advanced varieties of artificial intelligence tasks [33, 13, 19]. Despite these tremendous success, newly developed networks tend to have more learnable parameters which also mean more floating-point operations (FLOPs). As a result, these DNNs can be rarely run on the general CPUs embedded devices with limited computation power [11]. By pruning the redundancy in DNNs, the emerging network sparsity has become a broad consensus in favour of model deployment by both the academe and industries.

As illustrated in Fig. 1, according to the basic pruning granularity, existing works accomplishing network sparsity are categorized into weight pruning and filter pruning. The basic granularity of weight pruning falls into individual weights at any location of the filters or connections between full-connected layers. It essentially sparsifies the network at a fine-grained level and is demonstrated to achieve an extremely high compression rate and high accuracy performance [11, 7, 29]. However, weight pruning receives very limited speed gains since its irregular sparsity barely takes advantage of vector processing architectures such as Single Instruction Multiple Data (SIMD), and poorly utilizes memory buses. In contrast, this increases latency due to the dependent sequences of reads [3]. Recent studies [38, 18, 3] advocated 2:4 sparsity where 2 out of 4 weights are zeros for every continuous 4 weights. Particularly, it achieved a  $2 \times$  speedup. However, the acceleration was realized

---

\*Corresponding Author: rrji@xmu.edu.cn

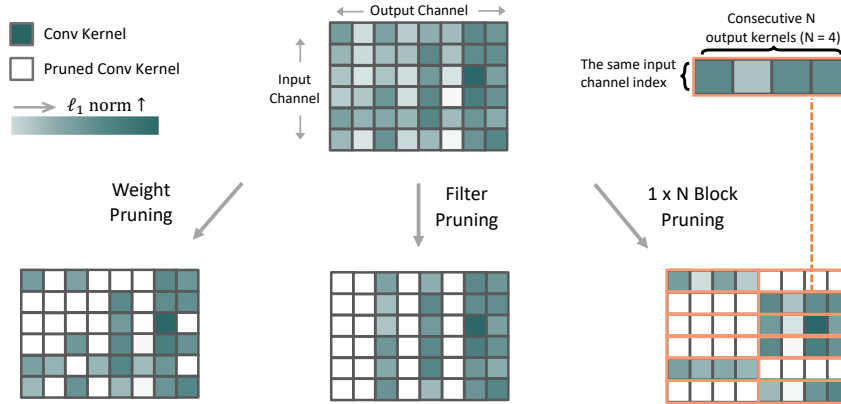


Figure 1: Comparison between existing pruning scenarios (weight pruning and filter pruning) and our  $1 \times N$  block pruning. Given a full model, weight pruning removes some weights in the filters and filter pruning removes the whole filters. In contrast, our  $1 \times N$  block pruning removes consecutive  $N$  output kernels with the same input channel index ( $N = 4$  in this illustration). Best view in colors.

on the specially designed sparse Matrix Multiply-Accumulate (MMA) instructions of NVIDIA A100 towards modern single- and multi-GPU workstations, servers, clusters, and even supercomputers [3], making it impossible to be utilized on other types of GPUs, let alone the CPUs-based platforms.

Different from weight pruning, the basic granularity of filter pruning in Fig. 1(b) consists of the whole filters. It implements network sparsity at a coarse-grained level by removing all weights in a filter. Consequently, the network structure does not change, thus the sparsified network can be well fitted by regular hardware and off-the-shelf basic linear algebra subprograms (BLAS) library to obtain acceleration. Nevertheless, filter pruning only maintains accuracy under moderate sparsity rates. Otherwise, such methods suffer more significant performance degradation than weight pruning methods. For example, a recent study [30] showed that a  $5.96 \times$  parameter reduction of ResNet-50 can well retain the accuracy performance of the original network by weight pruning, however, it is only a  $1 \times$  reduction in the case of filter pruning. Though the research community has developed varieties of techniques [22, 26, 9, 23], recent works [27, 20] demonstrated that the capacity of these techniques for performance improvement is indeed limited if appropriate training settings are given to the previous works. Therefore, how to simultaneously retain the performance and achieve apparent acceleration on mobile and embedded devices becomes a challenging but valuable problem. To our best knowledge, no method has ever been described to solve this problem so far.

In this paper, for the first time, we propose one novel pattern of  $1 \times N$  block sparsity (block pruning) with its merits in realizing both high-performing accuracy and apparent CPUs acceleration for practical model deployment. Our block pruning provides an intermediate granular level for network sparsity, which is coarser as compared to the fine-grained weight but finer as compared to the coarse-grained filter. An example of our sparsity pattern that satisfies  $N = 4$  requirement is shown in Fig. 1: the core distinction of our block pruning from existing scenarios [23, 26, 22] lies in that our basic pruning granularity is a block consisting of consecutive  $N$  output kernels with the same input channel index. In short, we aim to remove these blocks with smaller  $\ell_1$  norms that are considered less important in [22]. Our block sparsity in this paper follows the typical three-step pipeline of network training, pruning blocks with smaller  $\ell_1$  norms, and fine-tuning the sparsified one to recover the performance. At the point of the second step, we further propose a workflow of filter rearrangement, which rearranges the weight matrix in the output channel dimension according to the  $\ell_1$  norm of each filter, based on which more influential blocks with larger  $\ell_1$  norms are observed for accuracy improvements. Then, the next-layer weights are similarly rearranged in the input channel dimension to ensure the same convolutional results. In contrast to earlier developments [34, 36, 35] that also explore removing kernels, we have a stronger requirement of continuity on the  $N$  removed kernels, with its benefit in acceleration because these consecutive kernels can be stored continuously in the memory cache and the convolution with the inputs can proceed using a block-wise vectorized operation in parallel as analyzed in Sec. 3.4.

We display multiple compression rates using the light-weight MobileNet-V1 [17], -V2 [31], and -V3 [16] on the challenging ILSVRC-2012 [4], and compare our  $1 \times N$  block pruning with weight pruning and filter pruning. The experiments suggest an obviously increasing accuracy performance compared with filter pruning, and apparent inference acceleration compared with weight pruning. For example, in the case of 50% sparsity and  $N = 4$ , our block pruning obtains around 3.0% improvements over filter pruning in the top-1 accuracy of MobileNet-V2. Meanwhile, it obtains 56.04ms inference savings on Cortex-A7 CPU compared to weight pruning which obtains no speedup.

This work addresses the problem of simultaneously maintaining accuracy and achieving speedups on the general CPUs to enable practical model deployment. The key contributions of this paper include: (1) One novel pattern of  $1 \times N$  block pruning for network sparsity. (2) A workflow of filter rearrangement for accuracy improvements. (3) Simultaneously maintaining high-performing accuracy and achieving apparent CPUs acceleration for the first time.

The remainder of this paper is organized as follows: We briefly discuss some relevant prior works in network sparsity in Sec. 2. Then, we present details of our  $1 \times N$  block pattern for network sparsity in Sec. 3. In Sec. 4, a discussion on the empirical evaluation of our method in comparison with weight pruning and filter pruning is presented. We finally conclude in Sec. 5, laying out some avenues for future research in our  $1 \times N$  sparsity pattern.

## 2 Related Work

Traditional network sparsity including weight pruning and filter pruning is a classical research topic. We briefly review some related works below.

**Weight Pruning.** Weight pruning dates back to Optimal Brain Damage [21] and Optimal Brain Surgeon [12], which prune weights based on the Hessian of the loss function. Despite their accuracy retaining, the second-order Hessian needs additional computation cost. Dong *et al.* [6] restricted the second order derivatives for a specific layer to enable tractable computation. Han *et al.* [11] proposed to recursively remove small-weight connectivity and retrain the  $\ell_2$ -regularized subnetwork to derive smaller weight values. Dynamic network surgery [10] performs pruning and splicing on-the-fly. The former compresses the network and the latter recovers the incorrect pruning. The lottery ticket hypothesis [8] randomly initializes a dense network and trains it from scratch. The subnets with high-weight values are extracted, and retrained with the initial weight values of the original dense model. Lin *et al.* [25] proposed a dynamic allocation of sparsity pattern and incorporated feedback signal to reactivate prematurely pruned weights.

**Filter Pruning.** The norm of filter weight such as  $\ell_1$ -norm [22] is often considered as an indicator of filter importance. Filters with smaller norms are considered unimportant and removed. He *et al.* [14] pruned the filter with  $\ell_2$ -norm criterion, but the pruned filters are changeable and endowed with the chance to be recovered during network training. Ding *et al.* [5] computed the changes in the next layer’s outputs to evaluate the impact of pruning the filters. Lin *et al.* [24] used the artificial-bee-colony-based evolutionary algorithm to automatically search for the best pruning structure for each layer. He *et al.* [15] leveraged reinforcement learning to sample many subnetworks from the original CNN for evaluation, and ultimately find the best compressed network. Liu *et al.* [26] adopted meta-learning to prune redundant filters. It trains a weight-generating meta-network in advance for subnetworks evaluation, and then searches for the best subnetwork.

**Discussion.** While a variety of approaches for network sparsity have been proposed, existing methods fail to either maintain accuracy or achieve apparent speedups on the general CPUs-based platforms. Thus, it is natural for researchers to go further on sparsifying neural networks. This motivates our search for designing one new sparsity pattern that enables general CPUs acceleration as well as maintains accuracy performance.

## 3 Methodology

In this section, we introduce the intuition of our method and present its implementation details. In order to simplify the explanations, we only talk about the convolutional layers as illustrations. However, our block pruning can also be applied to the fully-connected layers since their weights can be regarded as  $1 \times 1$  convolutions.

### 3.1 Preliminaries

We start with notation definitions. Given a pre-trained  $L$ -layer CNN model  $F$ , we denote its filter set as  $\mathbf{W} = \{\mathbf{W}_j^i\}_{j=1}^{n^i}$  with  $\mathbf{W}^i = \{\mathbf{W}_j^i\}_{j=1}^{n^i} \in \mathbb{R}^{n^i \times m^i \times h^i \times w^i}$ , where  $n^i$ ,  $m^i$ ,  $h^i$  and  $w^i$  respectively denote the number of output channel, input channel, kernel height and width in the  $i$ -th layer;  $\mathbf{W}^i$  is the filter set for the  $i$ -th layer and  $\mathbf{W}_j^i$  is the  $j$ -th filter in the  $i$ -th layer. For the fully-connected layer, its weight matrix is an exception of  $h^i = 1$  and  $w^i = 1$ .

Network sparsity can be implemented by imposing a mask  $\mathbf{T}^i$  upon  $\mathbf{W}^i$ . Here  $\mathbf{T}^i$  is a binary tensor (0 or 1) with its entries indicating the states of network connections, *i.e.*, whether the corresponding weights are pruned or not. Thus, given an expected sparsity rate  $p$ , network sparsity is formally expressed as:

$$\arg \max_{\mathbf{T}^i} \mathcal{L}(\mathbf{W}^i \oplus \mathbf{T}^i), \quad s.t. \quad \frac{\|\mathbf{T}^i\|_0}{K} = 1 - p, \quad (1)$$

where  $\oplus$  represents the masking operation,  $\mathcal{L}(\cdot)$  measures the importance of its input, and  $K$  denotes the size of  $\mathbf{T}^i$  that varies according to the basic pruning granularity. We measure the input importance using the  $\ell_1$  norm of the basic pruning granularity. We find this criterion sufficient, however, other metrics, such as weight gradients [29], activation sparsity [28], can be adopted as well.

**Weight Pruning** removes individual weights at any location of  $\mathbf{W}^i$ . Thus, each mask  $\mathbf{T}^i$  has the same shape with  $\mathbf{W}^i$  of  $\mathbb{R}^{n^i \times m^i \times h^i \times w^i}$  and its size  $K = n^i \cdot m^i \cdot h^i \cdot w^i$ . The specific objective of weight sparsity is:

$$\arg \max_{\mathbf{T}^i} \sum_j^{n^i} \sum_k^{m^i} \sum_q^{h^i} \sum_r^{w^i} \mathcal{L}(\mathbf{W}_{j,k,q,r}^i \cdot \mathbf{T}_{j,k,q,r}^i), \quad s.t. \quad \frac{\|\mathbf{T}^i\|_0}{K} = 1 - p. \quad (2)$$

**Filter Pruning** removes the entire filter  $\mathbf{W}_j^i$ . Thus, each mask  $\mathbf{T}^i$  has the shape of  $\mathbb{R}^{n^i}$  and  $K = n^i$ . The specific objective of filter sparsity is:

$$\arg \max_{\mathbf{T}^i} \sum_{j=1}^{n^i} \mathcal{L}(\mathbf{W}_j^i \cdot \mathbf{T}_j^i), \quad s.t. \quad \frac{\|\mathbf{T}^i\|_0}{K} = 1 - p. \quad (3)$$

In the following, we introduce one novel concept of  $1 \times N$  block sparsity, whose basic pruning granularity falls into a series of blocks consisting of consecutive  $N$  output kernels with the same input channel index. We show that our block sparsity provides an efficient and effective alternative to simultaneously accelerate the model inference on modern CPUs-based platform and retain the accuracy performance.

### 3.2 $1 \times N$ Block Sparsity

We define the problem of pruning a neural network using our  $1 \times N$  block sparsity. In order to simplify the explanations, we reformat the representation of  $\mathbf{W}^i \in \mathbb{R}^{n^i \times m^i \times h^i \times w^i}$  as  $\mathbf{\Omega}^i \in \mathbb{R}^{m^i \times n^i}$ . Note that each element in  $\mathbf{\Omega}^i$  is a kernel with the shape of  $h^i \times w^i$ , *i.e.*,  $\mathbf{\Omega}_{k,j}^i = \mathbf{W}_{j,k,:}^i$ . Each column  $\mathbf{\Omega}_{:,j}^i$  stands for a filter and each row  $\mathbf{\Omega}_{k,:}^i$  consists of these kernels that have the same input channel index of  $k$ .

As shown in Fig. 1, we further partition the whole  $\mathbf{\Omega}^i$  into a collection of smaller blocks. Our partition can be made more precise for an  $m^i \times n^i$  matrix  $\mathbf{\Omega}^i$  by partitioning  $m^i$  into a collection of  $m^i$  row-groups, and then further partitioning  $n^i$  into a collection of  $\frac{n^i}{N}$  col-groups. Consequently, each block  $(k, j)$  is a  $1 \times N$  matrix including consecutive  $N$  output kernels with the same input channel index  $k$ , namely  $\mathbf{\Omega}_{k,(j-1) \cdot N + 1 : j \cdot N}^i$ . Based on this partitioned matrix, the basic pruning granularity of our  $1 \times N$  sparsity falls into these blocks. Thus, the mask,  $\mathbf{T}^i$ , in our  $1 \times N$  block sparsity has the shape of  $\mathbb{R}^{m^i \times \frac{n^i}{N}}$  and its size  $K = m^i \cdot \frac{n^i}{N}$ . Finally, the specific objective of our  $1 \times N$  block sparsity is:

$$\arg \max_{\mathbf{T}^i} \sum_{k=1}^{m^i} \sum_{j=1}^{\frac{n^i}{N}} \mathcal{L}(\mathbf{\Omega}_{k,(j-1) \cdot N + 1 : j \cdot N}^i \cdot \mathbf{T}_{k,j}^i), \quad s.t. \quad \frac{\|\mathbf{T}^i\|_0}{K} = 1 - p. \quad (4)$$

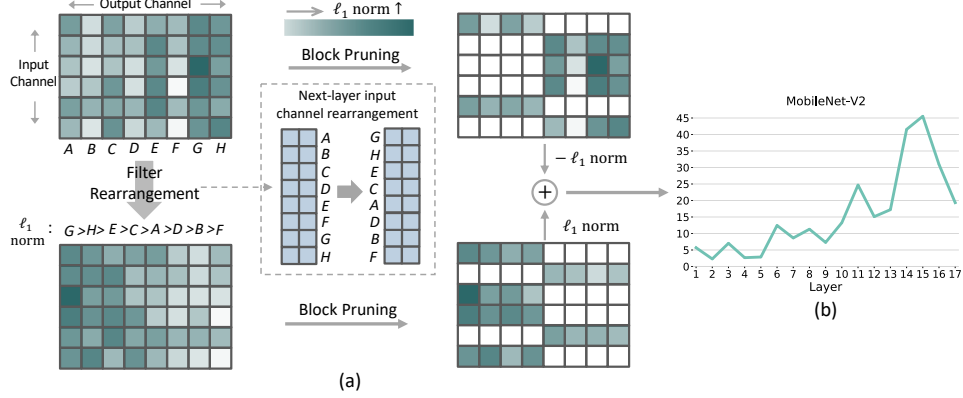


Figure 2: Workflow of filter rearrangement. We rearrange the weight matrix in the output channel dimension using the  $\ell_1$  norm of each filter. Then, similar rearrangement is applied to the next-layer weight matrix in the input channel dimension. As results, more influential blocks with larger  $\ell_1$  norms are preserved for accuracy improvements, as validated using MobileNet-V2. Best view in colors.

Furthermore, we realize that weight pruning and filter pruning are two special cases of our proposed  $1 \times N$  block pattern. Specifically, our block pruning degenerates to weight pruning subject to  $N = 1$ ,  $h^i = 1$  and  $w^i = 1$ . Besides, it further degenerates to filter pruning if  $N = n^i$ . When  $1 < N < n^i$ , our method provides an intermediate granular level for network sparsity, since it is coarser as compared to the fine-grained weight pruning but finer as compared to the coarse-grained filter pruning. Many previous researches [34, 36, 35] also explore removing kernels; however, our block pruning has a stronger requirement of continuity on the  $N$  removed kernels, with its merits in acceleration since these consecutive kernels can be stored continuously in the memory cache and the convolution with the inputs can proceed using a parallelized block-wise vectorized operation as analyzed in Sec. 3.4. Therefore, it is expected that our block pruning can offer a better performance than the filter pruning, and also an apparent inference speedup comparing to the weight pruning.

### 3.3 Filter Rearrangement

Our  $1 \times N$  block sparsity in this paper follows the typical three-step pipeline of network training, then pruning blocks with smaller  $\ell_1$  norms, and fine-tuning the sparse one to recover the performance in the end. At the second pruning step, the opportunity exists to change the layout of the weight matrix  $\Omega^i$  to further relieve the pruning impact.

To implement the above process, we propose a workflow of filter rearrangement, whose working principle is shown in Fig. 2. Given the original weight matrix  $\Omega^i$  in the top-left of (a), simply applying  $1 \times N$  block sparsity upon  $\Omega^i$  leads to the loss of some blocks with relatively large values of  $\ell_1$  norms in the top-right of (a). We calculate the  $\ell_1$  norm of each filter, *i.e.*, one column in  $\Omega^i$ , then rearrange  $\Omega^i$  in the output channel dimension according to the calculated filter norm in a decreasing order as shown in the lower-left of (a). The rearranged weight matrix is denoted as  $\tilde{\Omega}^i$  to which our  $1 \times N$  block sparsity is further applied. As a consequence, more blocks with larger  $\ell_1$  norms are preserved after pruning in the lower-right of (a), leading to an overall increasing weight magnitude as verified on MobileNet-V2 of (b). The filter rearrangement requires the outputs to be similarly rearranged as well, so as to maintain the same convolutional results with the next-layer weight matrix. However, frequently rearranging outputs incurs more run-time cost in the inference. Alternatively, we choose to apply similar rearrangement to the input channel dimension of the next-layer weight matrix as illustrated in the middle of (a), which is accomplished once for all before pruning and thus brings no run-time cost. The effectiveness of filter rearrangement for accuracy improvements is presented in Sec. 4.

Then, Eq. (4) after filter rearrangement is reformulated as:

$$\arg \max_{\mathbf{T}^i} \sum_{k=1}^{m^i} \sum_{j=1}^{\frac{n^i}{N}} \mathcal{L}(\tilde{\Omega}_{k,(j-1) \cdot N + 1 : j \cdot N}^i \cdot \mathbf{T}_{k,j}^i), \quad s.t. \quad \frac{\|\mathbf{T}^i\|_0}{K} = 1 - p. \quad (5)$$

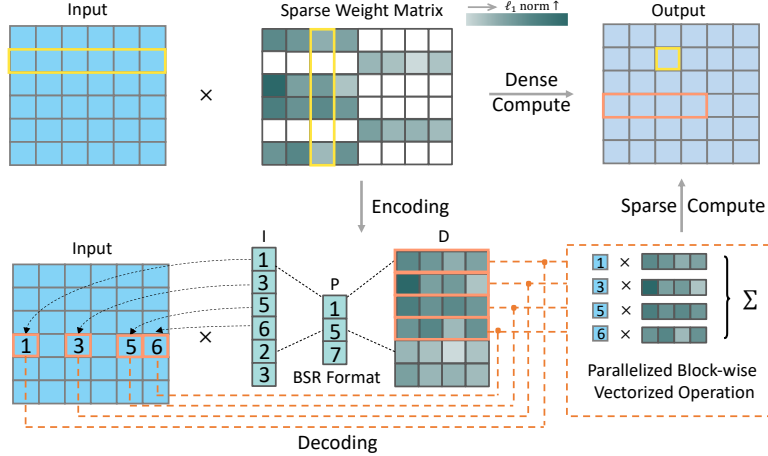


Figure 3: Encoding and Decoding of our  $1 \times N$  block sparsity. Our pruning pattern results in a sparse matrix with constant-size blocks, enabling it to be encoded by Block Compressed Sparse Row Format (BSR) to save the memory storage. In the decoding process, we calculate the outputs in a block-wise manner where the block-wise vectorized operation is applied in parallel to realize practical speedups. Best view in colors.

Note that the maximization of the above objective can be achieved by setting to 1s the entries of  $\mathbf{T}^i$  corresponding to these blocks in  $\tilde{\Omega}^i$  with their  $\ell_1$  norms within the largest top- $(1-p)$ , and 0s otherwise. As a consequence, the sparse weights after applying our  $1 \times N$  block pattern is then derived as:

$$\bar{\Omega}^i = \tilde{\Omega}^i \oplus \mathbf{T}^i. \quad (6)$$

### 3.4 Encoding and Decoding Efficiency

Given the input activation tensor  $\mathbf{X}^i$  as illustrated in Fig. 3, the output tensor  $\mathbf{Y}^i$  calculated by the standard dense-matrix structure is obtained as:

$$\mathbf{Y}_{k,j}^i = \sum_{z=1}^{m^i} \mathbf{x}_{k,z}^i \bar{\Omega}_{z,j}^i. \quad (7)$$

Considering a sparse matrix, operations using the standard dense-matrix structure bear inefficiency as processing and memory are wasted on a large number of zero-valued elements. Thus, it is of great necessity to take advantage of specialized data structures in order to store and manipulate the sparse matrix. However, the irregular sparse matrix resulting from weight pruning requires a great many of indices to record the positions of the reserved weights. Though Compressed Sparse Row Format (CSR) can be used to save index storage, irregular sparsity barely takes advantage of vector processing architectures and memory buses, resulting in little acceleration and even speed deterioration.

In contrast, due to the requirement of continuity on the  $N$  removed kernels, our pruning pattern results in a sparse matrix  $\bar{\Omega}^i$  with constant-sized blocks. This good property brings two merits: First, the constant-sized blocks are by nature more easily encoded by Block Compressed Sparse Row Format (BSR) [32] to save non-zero elements in  $\bar{\Omega}^i$  with significantly less storage for the indices. Second, the output tensor  $\mathbf{Y}^i$  is derived using a block-wise vectorized operation in parallel to achieve an apparent speedup. Specifically, as illustrated in Fig. 3, the sparse weight matrix  $\bar{\Omega}^i$  in our block pruning is encoded by BSR into three components: 1)  $\mathbf{D}^i \in \mathbb{R}^{t \times N}$ , 2)  $\mathbf{I}^i \in \mathbb{R}^t$  and 3)  $\mathbf{P}^i \in \mathbb{R}^{\frac{m^i}{N}+1}$ , where  $t$  is the number of non-zero blocks in  $\bar{\Omega}^i$ . The matrix,  $\mathbf{D}^i$ , and vector,  $\mathbf{I}^i$ , contain non-zero blocks and their row indices in  $\bar{\Omega}^i$ , respectively. We form  $\mathbf{D}^i$  by firstly stacking up non-zero blocks within the same col-group of  $\bar{\Omega}^i$ , and concatenating the stacked ones across different col-groups. The vector  $\mathbf{I}^i$  records the row index of each block item in  $\bar{\Omega}^i$ . The  $k$ -th element of the vector  $\mathbf{P}^i$  encodes the start row index of the  $k$ -th col-group in  $\mathbf{D}^i$ . The last element of  $\mathbf{P}^i$  is a fictitious index,

Table 1: Performance studies of our  $1 \times N$  block sparsity with and without filter rearrangement. The experiment is conducted using MobileNet-V2 with the pruning rate  $p = 50\%$ .

	$N = 2$ (%)		$N = 4$ (%)		$N = 8$ (%)		$N = 16$ (%)		$N = 32$ (%)	
	Top-1	Top-5	Top-1	Top-5	Top-1	Top-5	Top-1	Top-5	Top-1	Top-5
w/o Rearrange	69.900	89.296	69.521	88.920	69.206	88.608	68.971	88.399	68.431	88.315
Rearrange	70.233	89.417	69.579	88.944	69.372	88.862	69.352	88.708	68.762	88.425

which is always equal to  $t + 1$ . Attributed to the block storage format of  $\mathbf{D}^i$ , we can calculate  $\mathbf{Y}^i$  in a block-wise manner during decoding as follows:

$$\mathbf{Y}_{k, (j-1) \cdot N+1:j \cdot N}^i = \sum_{z=\mathbf{P}_{j/N}^i}^{\mathbf{P}_{j/N+1}^i-1} \mathbf{X}_{k, \mathbf{I}_z^i}^i \cdot \mathbf{D}_{\mathbf{I}_z^i}^i. \quad (8)$$

With proper index vectors  $\mathbf{P}^i$  and  $\mathbf{I}^i$ , we can directly fetch these activations corresponding to non-zero weights for the output computation, through which we avoid a complete involvement of the whole activation tensor as with the dense-matrix structure. Besides, the block storage format of  $\mathbf{D}^i$  also allows fast row data access since each block  $\mathbf{D}_{\mathbf{I}_z^i}^i$  is stored continuously in the memory. Moreover, the block-wise vectorized operation in Eq. (8) can be implemented extremely fast as the multiplication between input item  $\mathbf{X}_{k, \mathbf{I}_z^i}^i$  and each entry of  $\mathbf{D}_{\mathbf{I}_z^i}^i$  can proceed in parallel. Therefore, our  $1 \times N$  block sparsity can enable apparent acceleration on the general CPUs-based platforms. To guarantee end-to-end execution efficiency, we utilize the optimizing compiler TVM [2] to enable optimal code generation. And based on Eq. (8), we use Ansor [37] for automated tensor program generation to search best sparse convolution implementation.

## 4 Experiments

### 4.1 Implementation Settings

For fair comparison, similar to our block pruning, we construct the compared baselines of weight pruning and filter pruning using  $\ell_1$  norm as the importance evaluation. Besides, given the expected pruning rate  $p$ , we simply remove per-layer weights/filters/blocks with their corresponding  $\ell_1$  norms within the smallest top- $p$ . All experiments are performed using the pre-trained light-weight MobileNet-V1 [17], -V2 [31], and -V3 [16] on ILSVRC-2012 [4] that contains over 1.2 million images for training and 50,000 validation images from 1,000 classes. After pruning, we fine-tune the sparse models for 90 epochs on two NVIDIA V100 GPUs with the settings: Stochastic Gradient Descent (SGD) optimizer with a momentum of 0.9, weight decay of  $4e-5$  and initial learning rate of 0.1 with a cosine annealing. The data augmentation includes random cropping and horizontal flipping.

### 4.2 Ablation Study

We first analyze the influence of filter rearrangement in Sec. 3.3. Tab. 1 compares the performance of our  $1 \times N$  block sparsity for pruning MobileNet-V2 with and without filter rearrangement. The pruning rate  $p$  is set to 50%. As can be seen, rearranging filters consistently enhances the accuracy performance in both the top-1 and top-5, even with various block size ( $N$ ). For example, the top-1 classification accuracy of pruned MobileNet-V2 with  $1 \times 16$  block sparsity is increased by 0.381% (69.352% with and 68.971% without filter rearrangement). To dive into a deeper analysis, by rearranging the weight matrix in the output channel dimension, more blocks with larger  $\ell_1$  norms are preserved after applying our  $1 \times N$  block pruning as validated in Fig. 2(b). These results well validate the effectiveness of filter rearrangement in boosting the performance of pruned models.

### 4.3 Performance Comparison

In this section, we compare the performance of our proposed block pruning with traditional weight pruning and filter pruning. We show that the advantages of our  $1 \times N$  block sparsity are reflected from two perspectives: 1) maintaining better accuracy than filter pruning, and 2) achieving apparent CPUs acceleration comparing to weight pruning.

Table 2: Performance comparison of our  $1 \times N$  block sparsity against weight pruning and filter pruning. The experiment is conducted using MobileNet-V1/-V2/-V3 and the pruning rate  $p = 50\%$ .

	MobileNet ( $p = 50\%$ )							
	V1 (%)		V2 (%)		V3-small (%)		V3-large (%)	
	Top-1	Top-5	Top-1	Top-5	Top-1	Top-5	Top-1	Top-5
Origin	71.154	89.834	71.737	90.452	67.225	87.351	74.280	91.928
Weight Pruning	70.764	89.592	71.146	89.872	66.376	86.868	72.897	91.093
Filter Pruning	65.348	86.264	66.730	87.190	59.054	81.743	69.137	89.097
$1 \times 2$ Block (Ours)	70.281	89.370	70.233	89.417	65.380	86.060	72.120	90.677
$1 \times 4$ Block (Ours)	70.052	89.056	69.706	89.165	64.465	85.495	71.935	90.458
$1 \times 8$ Block (Ours)	69.908	89.027	69.372	88.862	64.101	85.274	71.478	90.163
$1 \times 16$ Block (Ours)	69.559	88.933	69.352	88.708	63.126	84.203	71.112	90.129
$1 \times 32$ Block (Ours)	69.541	88.801	68.762	88.425	62.881	83.982	70.769	89.696

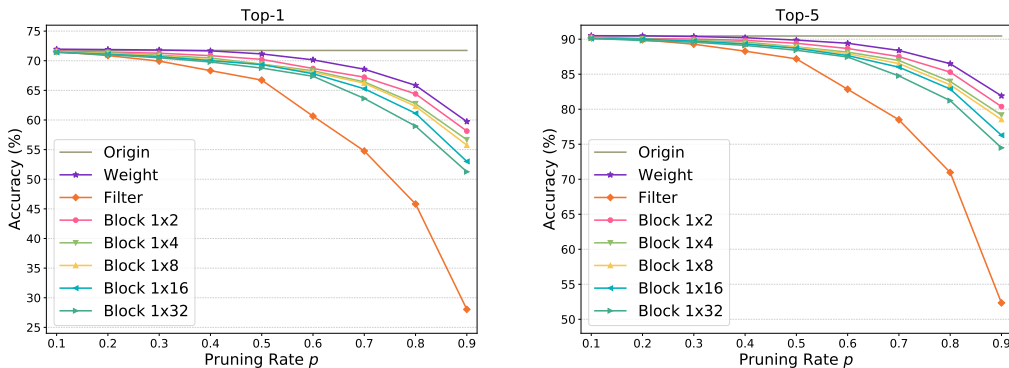


Figure 4: Performance comparison of our  $1 \times N$  block sparsity against weight pruning and filter pruning under different pruning rates. The experiment is conducted using MobileNet-V2. Best view in colors.

**Accuracy Performance.** We first study the performance of  $1 \times N$  sparsity across different networks. Tab. 2 displays the pruning results of our block pruning and existing weight pruning and filter pruning using MobileNet-V1/-V2/-V3 with the pruning rate  $p$  set to 50%. Tab. 2 shows that filter pruning suffers the most performance degradation of 5.806%, 5.007%, 8.171%, and 5.143% when pruning MobileNet-V1, V2, V3-small and V3-large, respectively. Such severe performance losses are attributed to its coarse-grained pruning granularity. Consequently, the poor performance barricades the using of filter pruning in practical model deployment. In contrast, due to its fine-grained pruning granularity, weight pruning presents the best performance with top-1 accuracy losses of 0.390%, 0.591%, 0.849%, and 1.383% when pruning MobileNet-V1, V2, V3-small and V3-large, respectively. Despite its ability to maintain high accuracy, weight pruning achieves rare acceleration as analyzed in the following. The poor speedup also disables the using of filter pruning. With respect to our proposed  $1 \times N$  block sparsity, we have two observations: 1) our method well boosts the performance of filter pruning regardless of the block size  $N$ . Taking MobileNet-V2 as an example, our  $1 \times 4$  block sparsity achieves 69.706% top-1 accuracy, significantly better than 66.730% of filter pruning. Though it is slightly poorer than 71.146% of weight pruning, our  $1 \times 4$  block sparsity obtains an apparent speedup as detailed in the following context. 2) The performance of  $1 \times N$  block sparsity degenerates as the block size  $N$  increases. The rationale behind this is that larger  $N$  indicates coarser pruning. As analyzed in Sec. 3.2, our block pruning degenerates to weight pruning with a small  $N$  and filter pruning with a large  $N$ .

Fig. 4 further shows the performance comparison when applying different pruning rates to sparsifying MobileNet-V2. We can see that the increasing pruning rate results in decreasing accuracy performance for all methods. However, filter pruning degenerates drastically if  $p > 50\%$ . In contrary, our block



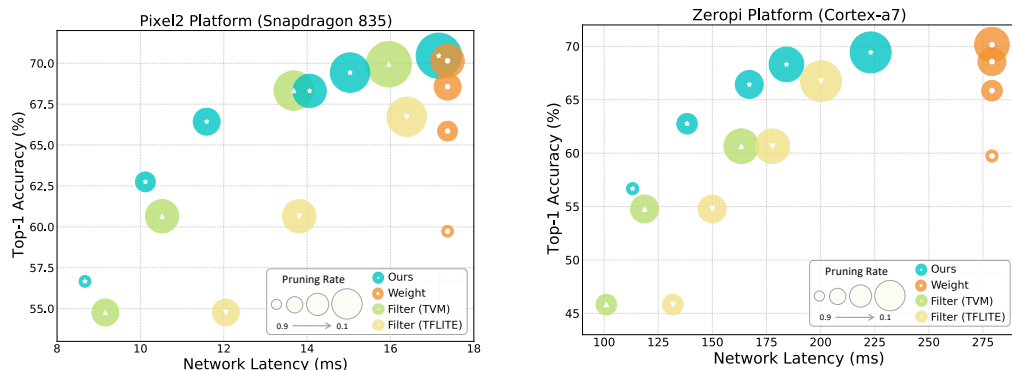


Figure 5: Performance and Latency comparison between our  $1 \times N$  ( $N = 4$ ) block sparsity against weight pruning and filter pruning. The experiment is conducted using MobileNet-V2 on the mobile platform of Pixel2 equipped with a Snapdragon 835 CPU (left), and the embedded platform of Zeropi equipped with a Cortex-a7 CPU (right). Best view in colors.

pruning maintains a similar decreasing tendency and close performance to weight pruning even if the pruning rate  $p$  is very high.

**CPUs Acceleration.** Fig. 5 presents the experimental results, which are conducted to further explore the acceleration capacity of different methods on CPUs-based platforms. In Sec. 3.4, we adopt TVM [2] to compile the pruned model of our block sparsity. For fair comparison, we also consider TVM compiler for weight pruning and filter pruning. Besides, additional experiments by TFLite compiler [1] are also presented for weight pruning and filter pruning. After model compiling, we respectively deploy the sparse models to obtain the practical network latency on the mobile platform of Pixel2 equipped with a Snapdragon 835 CPU and the embedded platform of Zeropi equipped with a Cortex-a7 CPU.

From Fig. 5, we observe no speedup from weight pruning, despite its ability to preserve good performance. As analyzed in Sec. 1, weight pruning leads to irregular sparsity that hardly utilizes the vector processing architectures and memory buses. Thus, weight pruning often results in little acceleration and even speed deterioration. Filter pruning leads to the most significant speedups since it does not modify the network structure, so that the pruned network can be well fitted by regular hardware to achieve acceleration. Nevertheless, the severe performance degradation disables the using of filter pruning in the model deployment. In contrast, our  $1 \times N$  ( $N = 4$ ) block sparsity achieves noticeable latency reductions across various pruning rates such as 56.04ms inference savings on Cortex-A7 CPU over weight pruning when  $p = 50\%$ , while maintaining comparable top-1 accuracy performance. Compared with weight pruning and filter pruning, our  $1 \times N$  block sparsity shows a better capacity of keeping a trade-off between latency reduction and performance retaining.

## 5 Conclusion and Future Work

This work proposed a novel concept of  $1 \times N$  block sparsity pattern to simultaneously maintain model accuracy and achieve significant speedups on general CPUs. Unlike previous approaches that prune a neural network at the granular level of the individual weights or the whole filters, we designed a block pruning that supports network sparsity by removing consecutive  $N$  output kernels with the same input channel index. To preserve more influential blocks, we proposed a workflow of filter rearrangement that rearranges the weight matrix in the output channel dimension and applies similar rearrangement to the next-layer weight matrix in the input channel dimension. Our sparsity pattern leads to a sparse matrix with constant-sized blocks enabling the computation outputs by using a parallelized block-wise vectorized operation. The experiments on the MobileNets and CPUs embedded hardware platforms demonstrated the effectiveness of our approach. Future research direction could implement our block pruning using the dynamic training manner to obtain accuracy gains. Besides, we plan to test block pruning on a wider variety of architectures to generalize applications of our method.

## Acknowledgement

This work is supported by the National Science Fund for Distinguished Young Scholars (No.62025603), the National Natural Science Foundation of China (No.U1705262, No.62072386, No.62072387, No.62072389, No.62002305, No.61772443, No.61802324 and No.61702136), Guangdong Basic and Applied Basic Research Foundation (No.2019B1515120049) and the Fundamental Research Funds for the central universities (No.20720200077, No.20720200090 and No.20720200091).

## References

- [1] Google llc. tensorflow lite. <https://www.tensorflow.org/lite>. [Online Accessed, 2019].
- [2] Tianqi Chen, Thierry Moreau, Ziheng Jiang, Lianmin Zheng, Eddie Yan, Haichen Shen, Meghan Cowan, Leyuan Wang, Yuwei Hu, Luis Ceze, et al. Tvm: An automated end-to-end optimizing compiler for deep learning. In *Symposium on Operating Systems Design and Implementation (OSDI)*, pages 578–594, 2018.
- [3] Jack Choquette, Wishwesh Gandhi, Olivier Giroux, Nick Stam, and Ronny Krashinsky. Nvidia a100 tensor core gpu: Performance and innovation. *IEEE Micro*, 41(02):29–35, 2021.
- [4] Jia Deng, Wei Dong, Richard Socher, Li-Jia Li, Kai Li, and Li Fei-Fei. Imagenet: A large-scale hierarchical image database. In *Proceedings of the IEEE/CVF Conference on Computer Vision and Pattern Recognition (CVPR)*, pages 248–255, 2009.
- [5] Xiaohan Ding, Guiguang Ding, Yuchen Guo, Jungong Han, and Chenggang Yan. Approximated oracle filter pruning for destructive cnn width optimization. In *Proceedings of the International Conference on Machine Learning (ICML)*, pages 1607–1616, 2019.
- [6] Xin Dong, Shangyu Chen, and Sinno Pan. Learning to prune deep neural networks via layer-wise optimal brain surgeon. In *Proceedings of the Advances in Neural Information Processing Systems (NeurIPS)*, pages 4860–4874, 2017.
- [7] Utku Evci, Trevor Gale, Jacob Menick, Pablo Samuel Castro, and Erich Elsen. Rigging the lottery: Making all tickets winners. In *Proceedings of the International Conference on Machine Learning (ICML)*, pages 2943–2952, 2020.
- [8] Jonathan Frankle and Michael Carbin. The lottery ticket hypothesis: Finding sparse, trainable neural networks. In *Proceedings of the International Conference on Learning Representations (ICLR)*, 2019.
- [9] Shaopeng Guo, Yujie Wang, Quanquan Li, and Junjie Yan. Dmcp: Differentiable markov channel pruning for neural networks. In *Proceedings of the IEEE/CVF Conference on Computer Vision and Pattern Recognition (CVPR)*, pages 1539–1547, 2020.
- [10] Yiwen Guo, Anbang Yao, and Yurong Chen. Dynamic network surgery for efficient dnns. In *Proceedings of the Advances in Neural Information Processing Systems (NeurIPS)*, pages 1379–1387, 2016.
- [11] Song Han, Jeff Pool, John Tran, and William Dally. Learning both weights and connections for efficient neural network. In *Proceedings of the Advances in Neural Information Processing Systems (NeurIPS)*, pages 1135–1143, 2015.
- [12] Babak Hassibi and David Stork. Second order derivatives for network pruning: Optimal brain surgeon. In *Proceedings of the Advances in Neural Information Processing Systems (NeurIPS)*, pages 164–171, 1992.
- [13] Kaiming He, Xiangyu Zhang, Shaoqing Ren, and Jian Sun. Deep residual learning for image recognition. In *Proceedings of the IEEE/CVF Conference on Computer Vision and Pattern Recognition (CVPR)*, pages 770–778, 2016.

- [14] Yang He, Guoliang Kang, Xuanyi Dong, Yanwei Fu, and Yi Yang. Soft filter pruning for accelerating deep convolutional neural networks. In *Proceedings of the International Joint Conference on Artificial Intelligence (IJCAI)*, pages 2234–2240, 2018.
- [15] Yihui He, Ji Lin, Zhijian Liu, Hanrui Wang, Li-Jia Li, and Song Han. Amc: Automl for model compression and acceleration on mobile devices. In *Proceedings of the European Conference on Computer Vision (ECCV)*, pages 784–800, 2018.
- [16] Andrew Howard, Mark Sandler, Grace Chu, Liang-Chieh Chen, Bo Chen, Mingxing Tan, Weijun Wang, Yukun Zhu, Ruoming Pang, Vijay Vasudevan, et al. Searching for mobilenetv3. In *Proceedings of the IEEE/CVF International Conference on Computer Vision (ICCV)*, pages 1314–1324, 2019.
- [17] Andrew G Howard, Menglong Zhu, Bo Chen, Dmitry Kalenichenko, Weijun Wang, Tobias Weyand, Marco Andreetto, and Hartwig Adam. Mobilenets: Efficient convolutional neural networks for mobile vision applications. *arXiv preprint arXiv:1704.04861*, 2017.
- [18] Itay Hubara, Brian Chmiel, Moshe Island, Ron Banner, Seffi Naor, and Daniel Soudry. Accelerated sparse neural training: A provable and efficient method to find n: M transposable masks. *arXiv preprint arXiv:2102.08124*, 2021.
- [19] Yoon Kim, Yacine Jernite, David Sontag, and Alexander M Rush. Character-aware neural language models. In *Proceedings of the AAAI Conference on Artificial Intelligence (AAAI)*, pages 2741–2749, 2016.
- [20] Duong Hoang Le and Binh-Son Hua. Network pruning that matters: A case study on retraining variants. In *Proceedings of the International Conference on Learning Representations (ICLR)*, 2021.
- [21] Yann LeCun, John Denker, and Sara Solla. Optimal brain damage. In *Proceedings of the Advances in Neural Information Processing Systems (NeurIPS)*, pages 598–605, 1989.
- [22] Hao Li, Asim Kadav, Igor Durdanovic, Hanan Samet, and Hans Peter Graf. Pruning filters for efficient convnets. In *Proceedings of the International Conference on Learning Representations (ICLR)*, 2016.
- [23] Mingbao Lin, Rongrong Ji, Yan Wang, Yichen Zhang, Baochang Zhang, Yonghong Tian, and Ling Shao. Hrank: Filter pruning using high-rank feature map. In *Proceedings of the IEEE/CVF Conference on Computer Vision and Pattern Recognition (CVPR)*, pages 1529–1538, 2020.
- [24] Mingbao Lin, Rongrong Ji, Yuxin Zhang, Baochang Zhang, Yongjian Wu, and Yonghong Tian. Channel pruning via automatic structure search. In *Proceedings of the International Joint Conference on Artificial Intelligence (IJCAI)*, pages 673–679, 2020.
- [25] Tao Lin, Sebastian U Stich, Luis Barba, Daniil Dmitriev, and Martin Jaggi. Dynamic model pruning with feedback. In *Proceedings of the International Conference on Learning Representations (ICLR)*, 2020.
- [26] Zechun Liu, Haoyuan Mu, Xiangyu Zhang, Zichao Guo, Xin Yang, Kwang-Ting Cheng, and Jian Sun. Metapruning: Meta learning for automatic neural network channel pruning. In *Proceedings of the IEEE/CVF International Conference on Computer Vision (ICCV)*, pages 3296–3305, 2019.
- [27] Zhuang Liu, Mingjie Sun, Tinghui Zhou, Gao Huang, and Trevor Darrell. Rethinking the value of network pruning. In *Proceedings of the International Conference on Learning Representations (ICLR)*, 2019.
- [28] Dmitry Molchanov, Arsenii Ashukha, and Dmitry Vetrov. Variational dropout sparsifies deep neural networks. In *Proceedings of the International Conference on Machine Learning (ICML)*, pages 2498–2507, 2017.
- [29] Pavlo Molchanov, Stephen Tyree, Tero Karras, Timo Aila, and Jan Kautz. Pruning convolutional neural networks for resource efficient inference. In *Proceedings of the International Conference on Learning Representations (ICLR)*, 2017.

- [30] Alex Renda, Jonathan Frankle, and Michael Carbin. Comparing rewinding and fine-tuning in neural network pruning. In *Proceedings of the International Conference on Learning Representation (ICLR)*, 2020.
- [31] Mark Sandler, Andrew Howard, Menglong Zhu, Andrey Zhmoginov, and Liang-Chieh Chen. Mobilenetv2: Inverted residuals and linear bottlenecks. In *Proceedings of the IEEE/CVF Conference on Computer Vision and Pattern Recognition (CVPR)*, pages 4510–4520, 2018.
- [32] Rukhsana Shahnaz and Anila Usman. Blocked-based sparse matrix-vector multiplication on distributed memory parallel computers. *The International Arab Journal of Information Technology (IAJIT)*, 8(2):130–136, 2011.
- [33] Yi Sun, Yuheng Chen, Xiaogang Wang, and Xiaoou Tang. Deep learning face representation by joint identification-verification. In *Proceedings of the Advances in Neural Information Processing Systems (NeurIPS)*, pages 1988–1996, 2014.
- [34] Mitchell Wortsman, Ali Farhadi, and Mohammad Rastegari. Discovering neural wirings. In *Proceedings of the Advances in Neural Information Processing Systems (NeurIPS)*, pages 2684–2694, 2019.
- [35] Saining Xie, Alexander Kirillov, Ross Girshick, and Kaiming He. Exploring randomly wired neural networks for image recognition. In *Proceedings of the IEEE/CVF International Conference on Computer Vision (ICCV)*, pages 1284–1293, 2019.
- [36] Jiaxuan You, Jure Leskovec, Kaiming He, and Saining Xie. Graph structure of neural networks. In *Proceedings of the International Conference on Machine Learning (ICML)*, pages 10881–10891, 2020.
- [37] Lianmin Zheng, Chengfan Jia, Minmin Sun, Zhao Wu, Cody Hao Yu, Ameer Haj-Ali, Yida Wang, Jun Yang, Danyang Zhuo, Koushik Sen, et al. Ansor: Generating high-performance tensor programs for deep learning. In *Symposium on Operating Systems Design and Implementation (OSDI)*, pages 863–879, 2020.
- [38] Aojun Zhou, Yukun Ma, Junnan Zhu, Jianbo Liu, Zhijie Zhang, Kun Yuan, Wenxiu Sun, and Hongsheng Li. Learning n:m fine-grained structured sparse neural networks from scratch. In *Proceedings of the International Conference on Learning Representation (ICLR)*, 2021.